February 1980 LRP 165/80

STATIONARY POTENTIAL JUMPS IN A PLASMA

Ch. Hollenstein, M. Guyot and E.S. Weibel

Stationary Potential Jumps in a Plasma

Ch. Hollenstein, M. Guyot and E.S. Weibel

Centre de Recherches en Physique des Plasmas

Association Euratom - Confédération Suisse

Ecole Polytechnique Fédérale de Lausanne

CH-1007 Lausanne / Switzerland

ABSTRACT

In a current-carrying plasma with $v_d < v_{Te}$ the existence of localized stationary potential jumps with $e\phi/kTe > 1$ is demonstrated. High-frequency ($<f_{pe}$) noise and low-frequency ($<f_{pi}$) noise with $W/nTe \approx .2$ peak around the transition region. Ion and electron heating is observed. High anomalous resistivity is found on the high potential side of the jump, with a maximum value within the jump.

In recent years it has been shown theoretically[1-4] and experimentally[5-8] that large potential gradients can exist in the plasma. It is known that the Buneman and Pierce instability induce the formation of potential jumps in an electron-beam plasma system.[8] Up to the present, from both theoretical and experimental results,[6,7] it was believed that a necessary condition for the formation of potential jumps was that the electron drift velocity v_d exceeded the electron thermal velocity v_{Te}.

In this report, we present for the first time experimental evidence for the existence of a stationary potential jump with $e\phi/kTe \approx 5$ in a current-carrying plasma in which the electron drift velocity v_d is only .2 v_{Te} ($v_{Te} = (8kT_e/\pi m)^{\frac{1}{2}}$).

The experiment was performed in a long cylindrical triple plasma device. The length and diameter of the stainless steel central section is 300cm and 20cm, respectively. The end sections are 30cm long and contain electron-emitting filaments to produce an argon plasma ($p = 4 \cdot 10^{-4}$ Torr). These end sections will be referred to as sources. The plasma drifts into the grounded central section through grids, guided by a magnetic field of 25 Gauss. A current can be established through the plasma

by biasing one of the sources and its grid (Fig. 1). In the absence of a current, typical operating parameters were $n_e \approx 2 \cdot 10^9$ cm^{-3}, $T_e \approx 1.2$ eV, $T_i \approx .2$ eV. The device has been operated in two different regimes. Under condition I the filaments inside the sources were heated to produce equal electron emission currents. Under condition II the filaments of the unpolarized source were cold.

The basic plasma parameters, such as the electron-density, the electron-temperature and the low-frequency fluctuations δn, were monitored by a small cylindrical Langmuir probe (diameter = .3mm). A movable probe consisting of two plane Langmuir probes facing opposite directions, was used to measure the electron drift velocity on axis, along the central section. The normalized drift velocity v_d/v_{Te} was obtained from the difference between the electron saturation currents of the two plane probes. The same probe was used to measure the upstream and downstream electron distribution functions $f_e(v)$. The up- and downstream ion temperatures were measured by a movable ion energy analyzer with an energy resolution of .1 eV. The local plasma potential along the axis was monitored by a small emissive probe. The low- ($<f_{pi}$) and high- ($<f_{pe}$) frequency spectra were recorded by a capacitive probe which is known[9,10] to have a flat frequency response up to frequencies around f_{pe} ($\approx$ 400-500 MHz). A Langmuir probe would draw a dc current which makes the recorded spectra meaningless.[11] A capacitive probe, however, does not suffer from this drawback.

The plasma potential along the central section is shown in Fig. 2a as a function of the biasing voltage V_g. The formation of potential jumps is observed for grid voltages higher than about 5V under condition I. For voltages higher than 30V even two or three jumps are created. The heights of the potential jumps are of the order of $e\phi/kT_e \approx 5$ and their width is typically 300-500 Debye-lengths. The electron-density profiles show a pronounced depression (20%) at the centre of the jumps. A more detailed study has been made for $V_g = 20V$, under conditions I and II (Fig. 2b). For condition II no potential step is formed; however a nearly-constant potential gradient is established. For both situations the measured value for the electron drift velocity remains of the order of $.2\ v_{Te}$ (Fig. 2c). In both cases an increase in the ion and electron temperature has been observed ($\Delta T_e \approx 2$ eV $\Delta T_i \approx .8$ eV). For frequencies below ω_{pi} the normalized turbulent wave energy $(\delta n/n)^2 = W/nT_e$ varies between 10^{-3} and .1 in case I and between 10^{-4} and .5 in case II. The fluctuation level in case I always peaks at the low potential foot of the potential jump. An increasing fluctuation peak moves towards the high potential side for an increasing V_g in case II. The frequency spectra show that, most of the turbulent wave energy is concentrated below $f_{pi}/2$. For high W/nT_e we observe an increase in the fluctuations at frequencies below 20 kHz. All the measured spectra indicate that there is no simple dependance on ω such as that proposed by

Kadomtsev.[12]

A high energy electron beam has been detected in case I, located near the jump, on the high potential side (Fig. 3). It is found that the measured beam energy agrees with the energy the electrons could gain as they cross the potential step. High-frequency fluctuations have been observed in that region. The spectrum is centered around f_{pe} and has a fullwidth of about .3 f_{pe}. A localized increase of the electron temperature ($\Delta T_e \approx$ 3-4 eV) in that region can be attributed to the thermalisation of the electron beam. None of these effects have been found in case II (Fig. 3).

Under both experimental conditions anomalous resistivity has been observed. However, the measured profiles for the effective collision frequency are different. In case II the effective collision frequency remains almost constant, at about 100 times the classical value ν_{cl} (Fig. 4a). The same value has also been found on the high potential side of the jump. On the low potential side, the effective collision frequency drops to about 10 times the classical value. However, a value up to 700 ν_{cl} has been found within the jump. At this location the effective mean free path ($\lambda \approx$ 1-2 cm) has been found to be much smaller than the width of the observed jump (L = 15-20 cm). Thus the region within the jump is dominated by turbulent collisions.

It is known from numerical simulations for sufficiently long systems, that the anomalous resistivity induced by the ion acoustic instability may lead to the formation of potential jumps.[4] These simulations have shown that, in a sufficiently long system with $v_d < v_{Te}$, the ion-acoustic instability gives rise to an anomalous resistivity, which may build up a dc potential leading to the formation of a potential jump. These results are compatible with our observations in case I. However, our experiment under conditions II indicates that even the presence of a high anomalous resistivity is not a sufficient condition to induce the formulation of potential jumps.

To scale the effective collision frequency, formulae of the type $\nu^* \alpha \omega_{pe} \cdot (W/nT_e)$ are often used.[13] In either case I or II our observations cannot be fitted to any such scaling laws (Fig. 4b). We conclude that a unique value of the resistivity cannot be assigned to a given set of plasma parameters and current densities.

We would like to thank Dr. J. Vaclavik, Dr. K. Appert and Dr. M.Q. Tran for many helpful suggestions.

This work was supported by the Swiss National Science Foundation, the Ecole Polytechnique Fédérale de Lausanne and by Euratom.

REFERENCES

1 L.P. Block, Cosmic Electrodynamics 3, 349 (1972)

2 G. Knorr and C.K. Goertz, Astrophys. Space Sci. 31, 209 (1974)

3 J.S. De Groot, C. Barnes, A.E. Walstead and O. Buneman, Phys. Rev. Lett. 38, 1283 (1977)

4 T. Sato and H. Okuda, Bull. Amerc. Phys. Soc. 24, 1046 (1979)

T. Sato and H. Okuda, Princeton University Report PPPL-1565

5 M.J. Schönhuber, Z. Angew. Phys. 15, 454 (1963)

6 B.H. Quon and A.Y. Wong, Phys. Rev. Lett. 37, 1393 (1976)

7 P. Coakley, N. Hershkowitz, R. Hubbard and G. Joyce, Phys. Rev. Lett. 40, 230 (1978)

P. Coakley and N. Hershkowitz, Phys. Fluids 22, 1171 (1979)

8 S. Iizuka, K. Saeki, N. Sato and Y. Hatta, Phys. Rev. Lett. 43, 1404 (1979)

9 J.A. Schmidt, Rev. Sci. Instr. 39, 1297 (1968)

10 J.R. Roth and W.M. Krawczonek, Rev. Sci. Instr. 42, 589 (1971)

11 W. Gekelman and R.L. Stenzel, Phys. Fluids 21, 2014 (1978)

12 B.B. Kadomtsev, Plasma Turbulence (Academic, New York, 1965)

13 R.Z. Sagdeev, Rev. Mod. Phys. 51, 1 (1979)

FIGURE CAPTIONS

Fig. 1 Schematic of the long triple plasma device.

Fig. 2 (a) Steady-state plasma potential versus position as a function of the grid bias V_g. The biased grid is located at the position x = 0.

(b) Steady-state plasma potential versus position for the two different operating regimes (case I and case II) of the device with V_g = 20V.

(c) Normalized electron drift velocity v_d/v_{Te} ($v_{Te} = (8kT_e/\pi m)^{\frac{1}{2}}$) versus position for case I and case II with V_g = 20V.

Fig. 3 Normalized turbulent wave energy $W/n\,T_e$ for frequencies below the ion plasma frequency as a function of distance for V_g = 20V. (Dotted line: corresponding potential profile). Power-spectra (linear scale) as measured by the capacitive probe at three different positions from the biased grid.

Fig. 4 High frequency noise for frequencies below the electron plasma frequency versus position with power spectra (linear scale) measured by the capacitive probe at three different positions from the biased grid, for V_g = 20V. (Dotted line: corresponding potential profile). Electron distribution functions $f_e(v)$ for the same three locations along the central section of the device.

Fig. 5 (a) The effective collision frequency ν^* versus position for the cases I and II. (Dotted line: corresponding potential profile).

(b) Effective collision frequency ν^* versus $\omega_{pe} \cdot (W/nT_e)$ in case I (●) and case II (0). (Dotted line: corresponding to the scaling law $\nu^* = \omega_{pe} \cdot (W/nT_e)$)

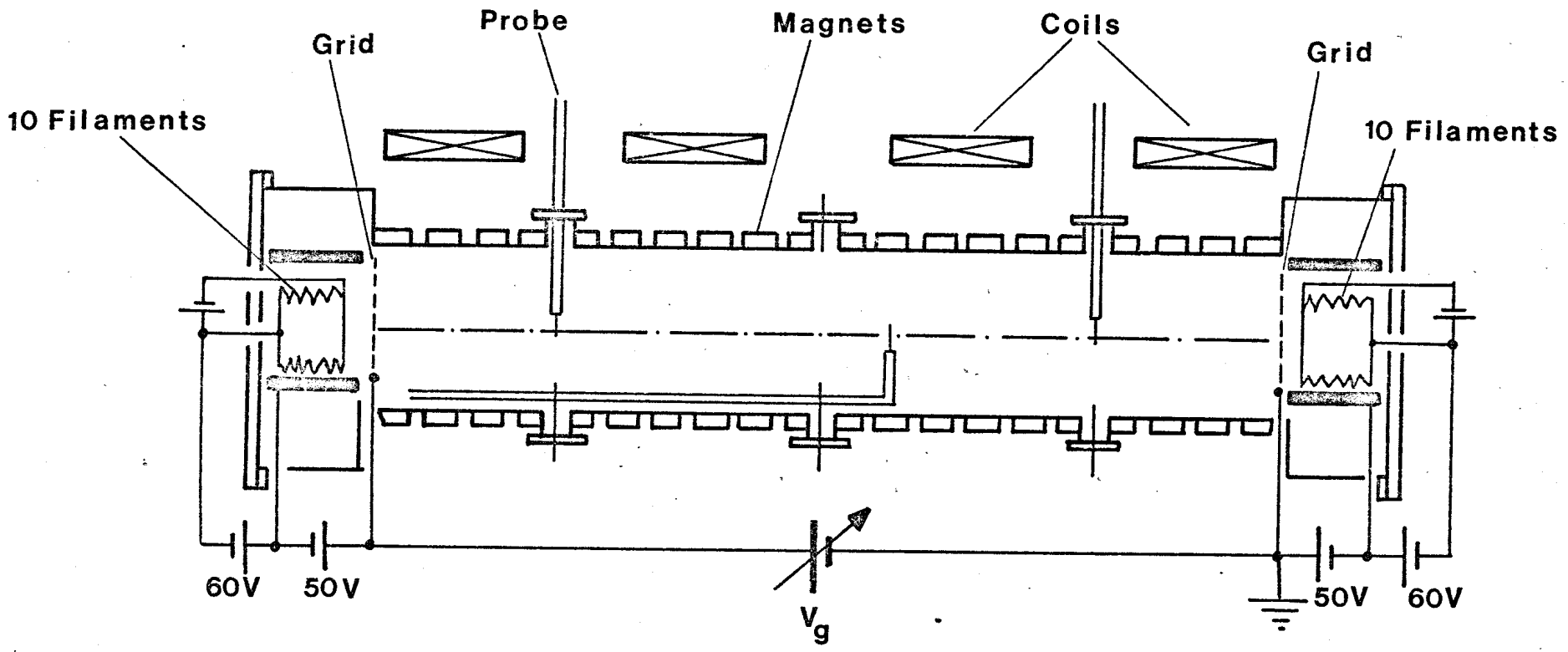

Fig. 1

Hollenstein et al

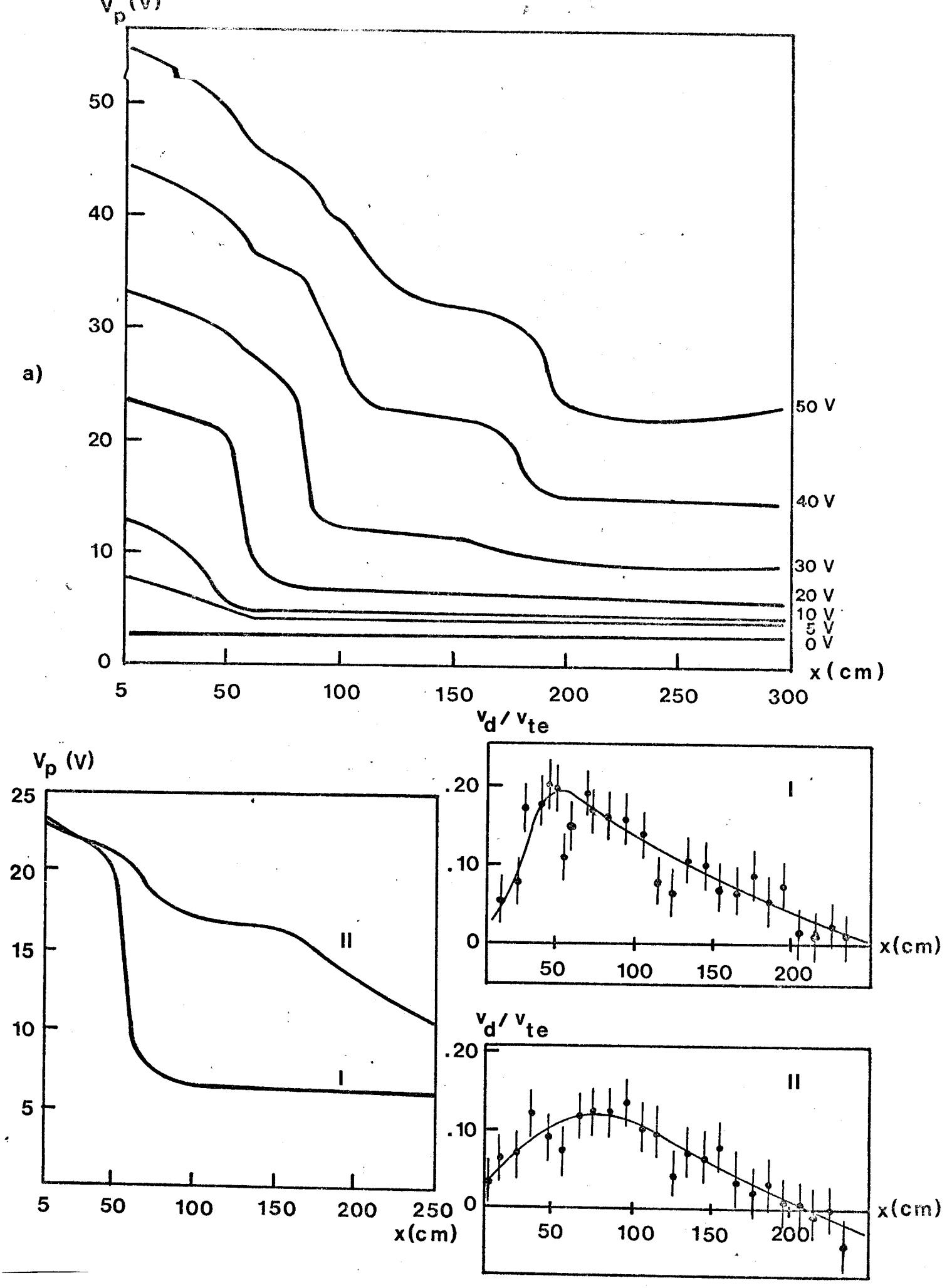

Fig. 2

Hollenstein et al

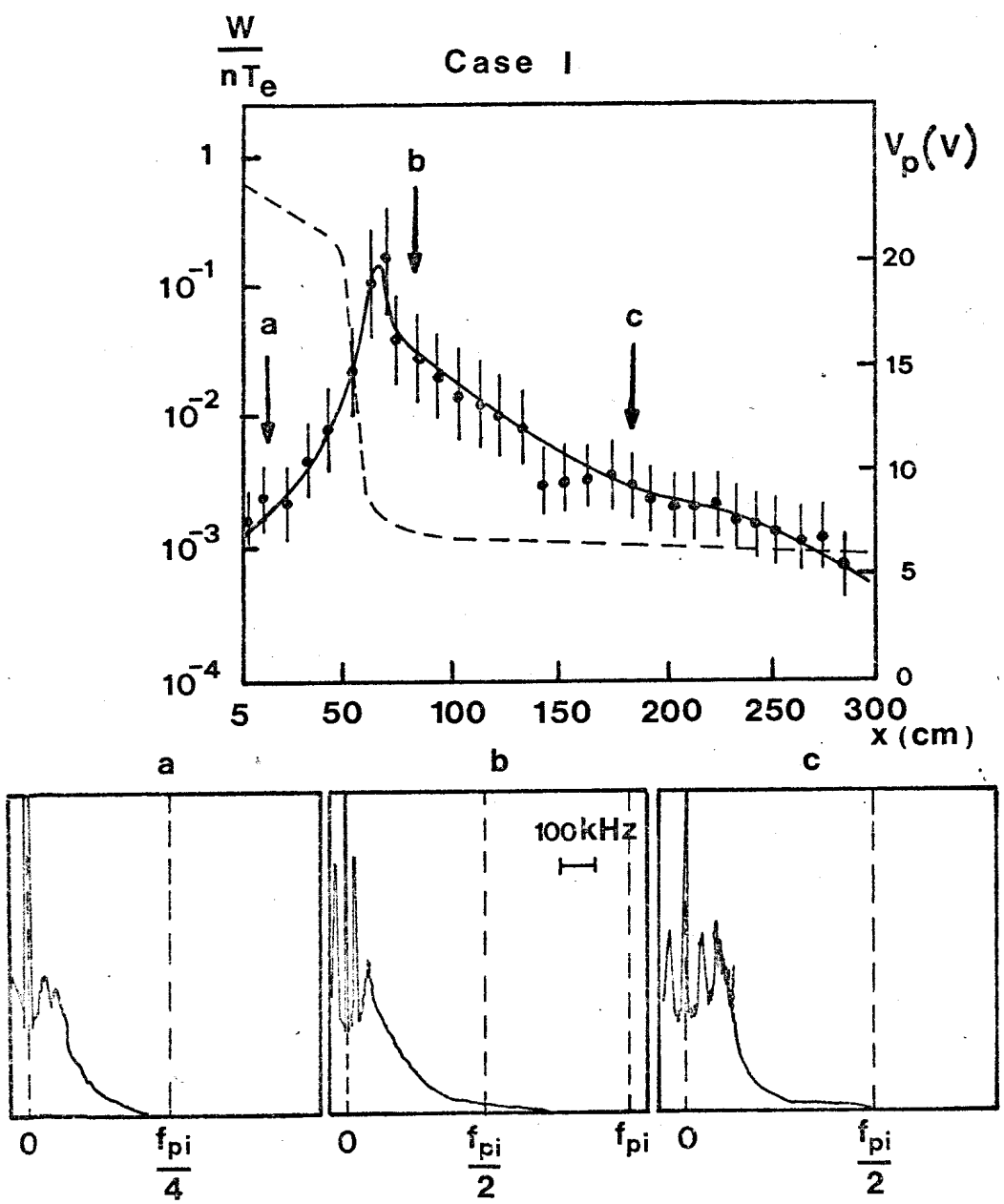

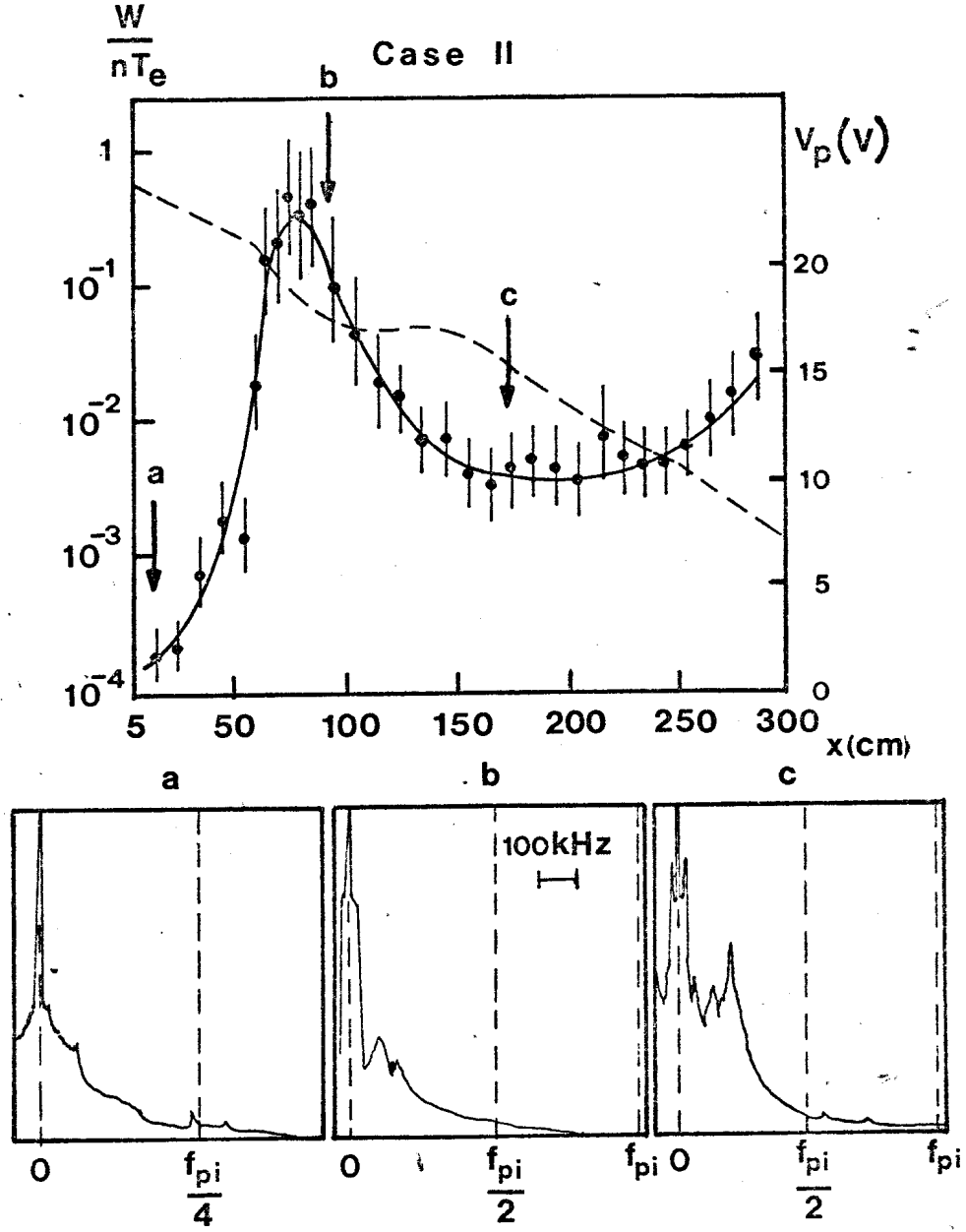

Fig. 3

Hollenstein et al

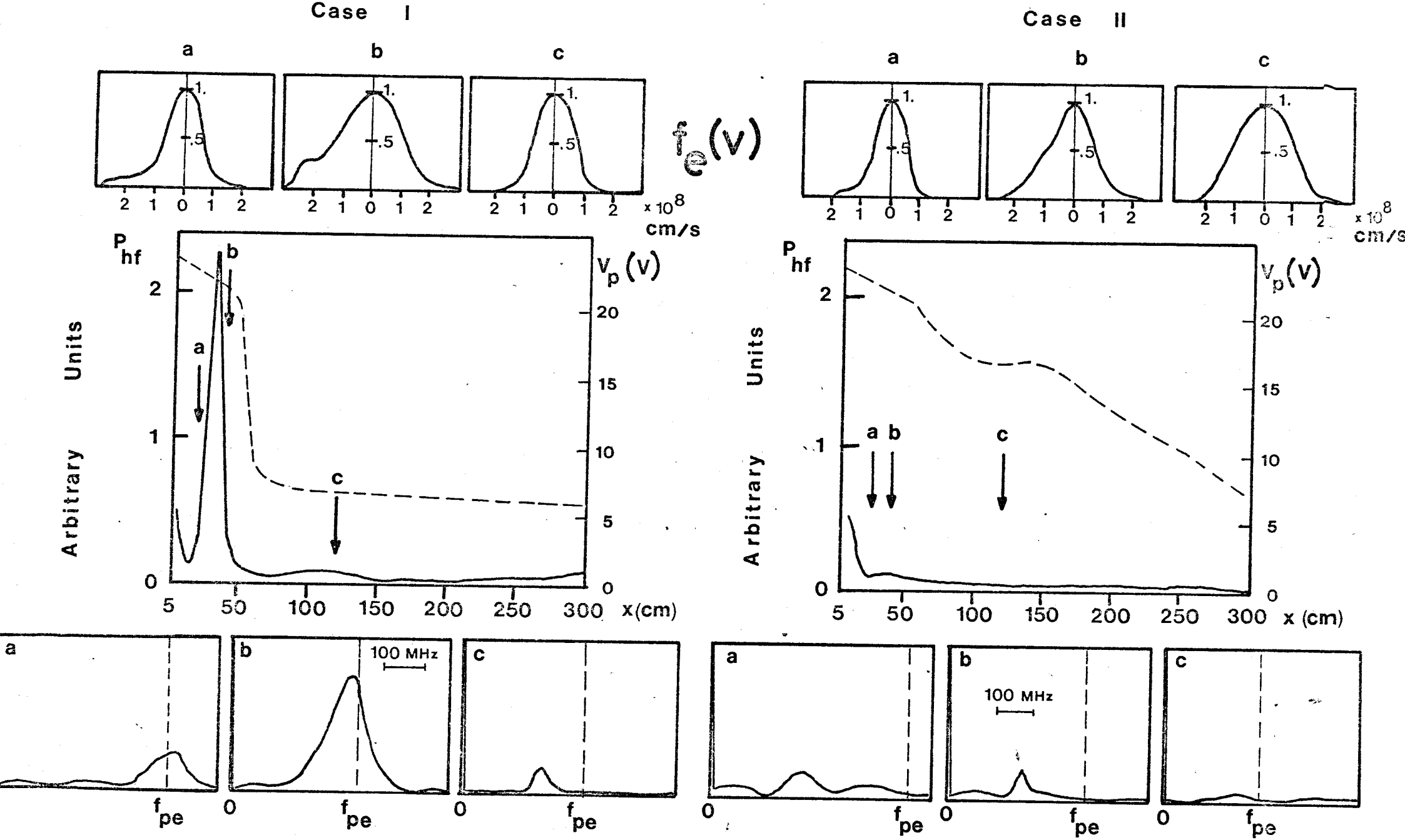

Fig. 4

Hollenstein et al

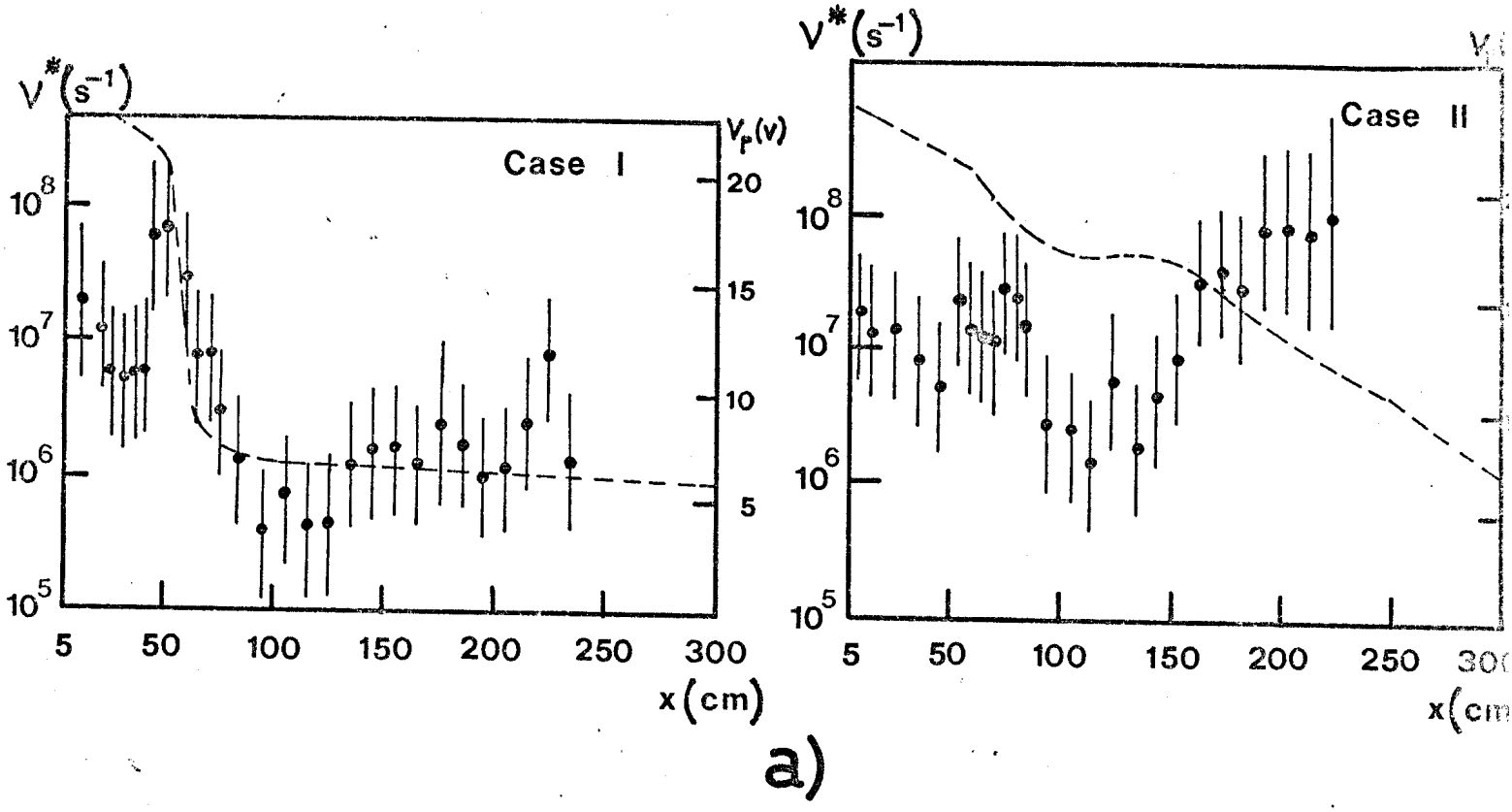

a)

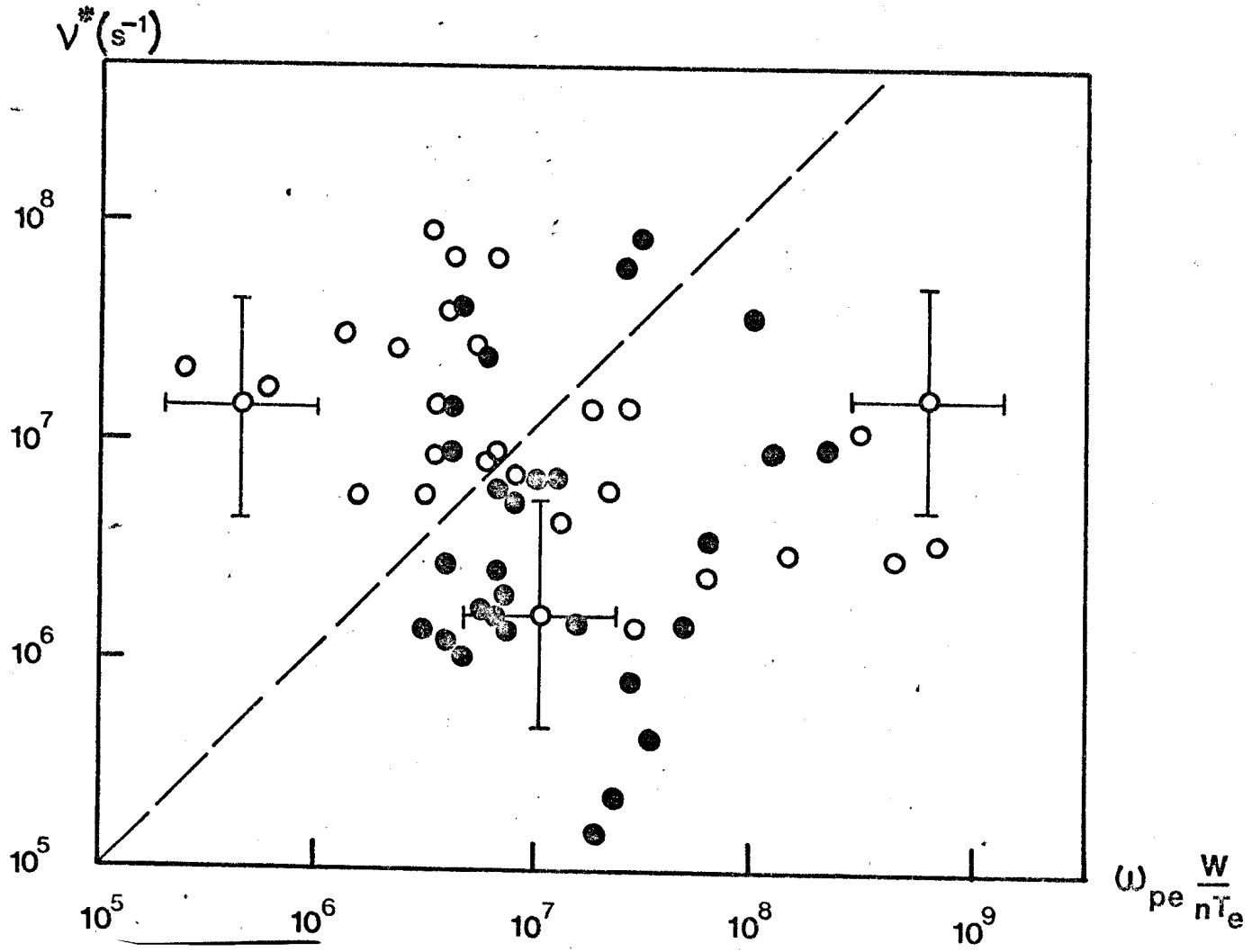

b)

Fig. 5
Hollenstein et al